IEEE Photonics Journal
An IEEE Photonics Society Publication

Open Access

Numerical Analysis on Polarization-Induced Doping III-Nitride n-i-p Solar Cells

Volume 7, Number 1, February 2015

Ya-Ju Lee
Yung-Chi Yao
Zu-Po Yang

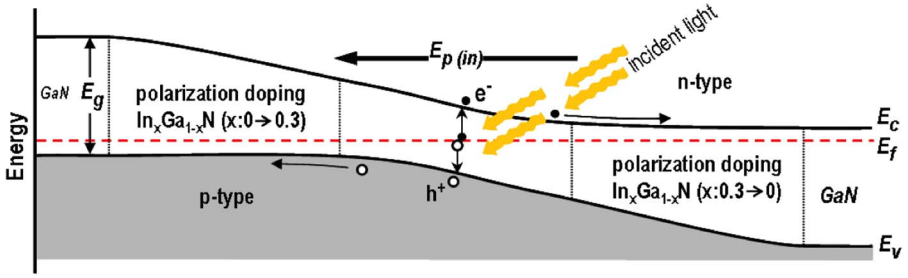

DOI: 10.1109/JPHOT.2015.2392374
1943-0655

IEEE photonics SOCIETY

IEEE

Numerical Analysis on Polarization-Induced Doping III-Nitride n-i-p Solar Cells

Ya-Ju Lee,[1] Yung-Chi Yao,[1] and Zu-Po Yang[2]

[1]Institute of Electro-Optical Science and Technology, National Taiwan Normal University, Taipei 116, Taiwan
[2]Institute of Photonic System, National Chiao Tung University, Tainan 711, Taiwan

DOI: 10.1109/JPHOT.2015.2392374

Manuscript received October 9, 2014; revised December 30, 2014; accepted January 7, 2015. Date of publication January 19, 2015; date of current version January 30, 2015. This work was supported by the National Science Council (NSC) of Taiwan under Contract MOST 103-2112-M-003-008-MY3, Contract MOST 104-2622-M-003-001-CC2, and Contract NSC 102-2218-E-009-017. Corresponding authors: Y.-J. Lee and Z.-P. Yang (e-mail: yajulee@ntnu.edu.tw; zupoyang@nctu.edu.tw).

Abstract: We design and numerically evaluate a new type of III-nitride n-i-p solar cells whose p- and n-type regions with equal carrier concentration of 3×10^{18} cm^{-3} are not generated by extrinsic impurity doping but by the so-called polarization-induced doping, which is induced by the graded $In_xGa_{1-x}N$ layers of linearly increasing (from $x = 0\%$ to 30%) and decreasing (from $x = 30\%$ to 0%) indium composition to construct the conductive p- and n-type regions, respectively. Because of the identical and uniform polarization charges within each unit cell, a smooth spatial variation of the potential profile of the device is, hence, expected, which mitigates the energy band discontinuities at heterointerfaces and facilitates transportation and collection of photogenerated carriers with high efficiency. Most importantly, as the conductive n- and p-type regions are formed by electrostatic field ionization but not by the thermal activation, the concentration of field-induced carriers is independent of thermal freeze-out effects. Thus, the polarization-induced doping III-nitride n-i-p solar cells can provide stable power conversion efficiency, even when operated at low temperatures.

Index Terms: Polarization-induced doping, III-nitride, n-i-p solar cells, wurtzite structure.

1. Introduction

Recently, most of research progress in III-nitride solar cells was mainly achieved by the double hetero-junction structures similar to the fundamental structures of III-nitride light-emitting diodes, i.e., the p-GaN/i-InGaN/n-GaN layers (from top to bottom) grown by the metal organic chemical vapor deposition (MOCVD), where an intrinsic InGaN layer or the multiple quantum-well (MQW) was sandwiched between p- and n-type GaN for the absorption of solar light [1]–[8]. For such a stacked p-i-n configuration, the epitaxial strain caused by the lattice-mismatch between the InGaN and GaN hetero-junctions is the most challenging issue, which limits the power conversion efficiency of the device. In addition to the material defects acting as trapping centers of photogenerated carriers, the epitaxial strain significantly hinders the efficient collections of photogenerated carriers because it induces piezoelectric polarization dipoles within the InGaN layer having electric field opposite to the direction of built-in electric field generated by typical p-n junction [9], [10]. Theoretically, rearranging the order of stacked layers as n-GaN/i-InGaN/p-GaN

structure can mitigate the adverse impact of piezoelectric effect since the polarization dipoles of absorption layer is now in the direction of depletion field. Yet, for the standard MOCVD equipped with impurity doping system, the growth of such a III-nitride n-i-p solar cell is practically infeasible due to the outgassing-prone of dopant acceptor (Mg) in p-GaN and its strong memory effect [11]. Additionally, in consideration of their high cost, potentially high conversion-efficiency [12], and large resistance of photon radiation [13], the main applications of III-nitride solar cells are possible for systems of the outer space, where the lowest temperature is down to a few degrees of Kelvin, depending on the areas of the space. Here another bottleneck is arisen from the large activation energy (E_A) of Mg dopant in p-GaN $(E_A \sim 200$ meV$)$ [14], [15], which is several times of the thermal energy of room temperature $(K_BT \sim 26$ meV$)$, and that constrains the thermal activation of acceptor according to the description of Arrhenius equation $[\text{GaN} : \text{Mg} \sim \exp(-E_A/K_BT)]$. Therefore, for a III-nitride solar cell used in the outer space, the carrier freezeout would lead to less energetic carriers and ineffective screening, causing severe ionized impurity scattering that decreases the carrier mobility. As a result, the decreased carrier mobility will reduce the diffusion length of minority carrier, as well as the device's efficiency.

In this work, we numerically evaluate the effect of polarization engineering in III-nitrides by grading the composition of InGaN materials to form a new type of n-i-p solar cells. In the absence of any impurity doping, our proposed device's built-in electric field across the absorption layer is equivalent of its polarization-induced electric field, beneficial for the electric drifting and efficient collection of photogenerated carriers. Furthermore, as the conductive n- and p-type regions are formed by electrostatic field ionization but not by the thermal activation [16]–[18], the concentration of field-induced carriers is irrelevant to temperature variations. Such polarization-induced doping III-nitride n-i-p solar cells can, hence, provide stable power conversion efficiency, even when operated at low temperatures.

2. Physical Mechanism and Device Structure

2.1. Polarization-Induced Doping

Fig. 1(a) schematically illustrates the physical mechanism of polarization-induced doping n-i-p solar cell. In the Ga-face [0001] III-nitride material, due to its noncentrosymmetric nature of wurtzite structure, the total polarization (P) can be expressed by the sum of spontaneous (P_{SP}) and piezoelectric (P_{PZ}) polarizations $P = P_{SP} + P_{PZ}$. Here, we define the P direction along the growth direction (i.e., z direction) as positive, and essentially, each unit cell of the material contains an electrical dipole. As plotted in Fig. 1(a), the red and black arrows are polarization charge dipoles in the top and bottom of every unit cell of the crystal, respectively. The direction and length of every arrow represent the polarity (up is positive, and down is negative) and magnitude of polarization charge dipoles, respectively. Because $P$of $In_xGa_{1-x}N$ (where x is the indium mole fraction) increases with the increasing of indium composition (x), thus by grading $In_xGa_{1-x}N$ layer (from GaN) with x increasing, the resulting unbalanced bound charge of any two neighboring unit cells is equal and negative, as shown in the blue regions of Fig. 1(a) and (b). The volume density of polarization charge of graded $In_xGa_{1-x}N$ layer is given by $\rho(z) = -\nabla \cdot P(z) = (\partial P/\partial x) \times (\partial x/\ \partial z) = -1.98 \times 10^{-5} \times (x_2 - x_1)/d$ [C/cm^3], where x_1 and x_2 denote the indium compositions at the ends of the graded layer with d in thickness. To satisfy Poisson equation and charge neutrality, equivalent holes provided from native defects, such as Ga vacancies and background intrinsic carriers [19], [20], are introduced into the graded $In_xGa_{1-x}N$ layer, which in turn lowers the Fermi level and results in a p-type conducting region. Similarly, by reversely grading the $In_xGa_{1-x}N$ layer to GaN, the positive polarization charges can be achieved [the pink regions shown in Fig. 1(a) and (b)], which pulls electrons from remote donor-like surface states into the reversely graded $In_xGa_{1-x}N$ layer [21], realizing an n-type doping. In this work, we numerically evaluate the characteristics of polarization-induced doping in III-nitride solar cell by linearly grading the indium composition of $In_xGa_{1-x}N$ (from $x = 0\%$ to $x = 30\%$ and back to 0% indium) to construct the device's p- and n-type regions in the absence of any impurity doping. An

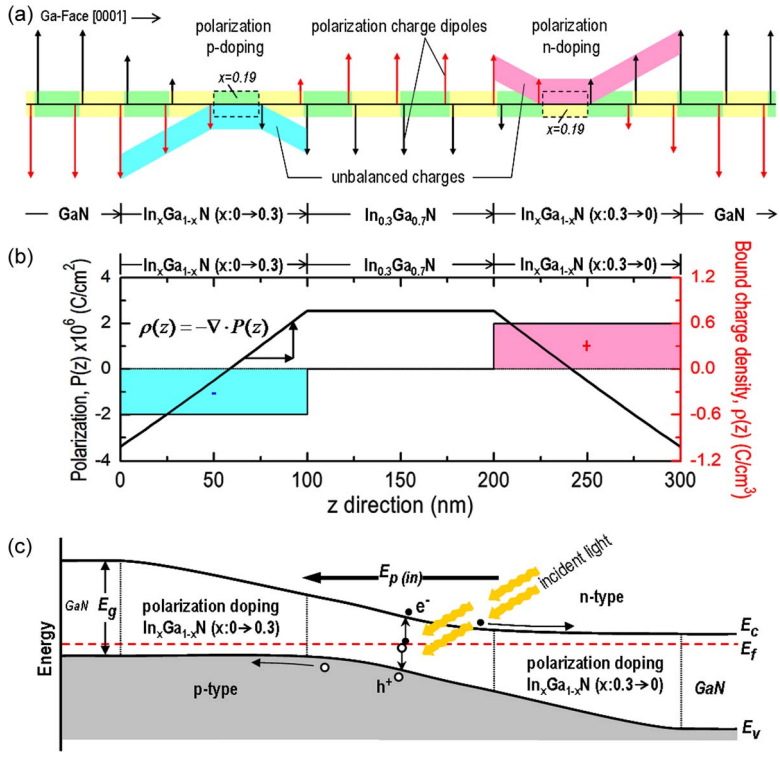

Fig. 1. Schematic illustration of polarization-induced doping III-nitride n-i-p solar cell by linearly grading the $In_xGa_{1-x}N$ layers. (a) Sheets of charge dipoles in every unit cell of the crystal. The alternating variation between yellow and green regions represents the arrangement of unit cells in the material. The unit cells denoting the $In_{0.19}Ga_{0.81}N$ material ($x = 0.19$, $P = 0$) are also marked in the figure. The orientation of polarization charge dipole (within a unit cell) switches its polarity after passing over the unit cell of $In_{0.19}Ga_{0.81}N$. (b) Net bound charge density given by $\rho(z) = -\nabla \cdot P(z)$ [C/cm^3]. (c) The corresponding energy-band diagram in a steady state, stressing the smooth potential profile without band offset for the efficient collection of photogenerated carriers.

$In_{0.3}Ga_{0.7}N$ layer serving as main absorption of solar light is inserted in the between of polarization-doping regions, as shown in Fig. 1(c). Accordingly, the varying range of x value which defines the device's polarization-induced doping region is mainly determined by the indium composition of the intrinsic absorption layer. In practice, due to fundamental thermodynamic limitations during growth of InGaN [22], it is difficult to obtain indium-rich (low band gap) absorption layer with high crystalline quality, and that is also the most challenging issue in the III-nitrides solar cells. Therefore, in this study, we set a reasonable indium composition in the absorption layer $(x = 30\%)$ with an achievable thickness (100 nm) by applying a compositionally graded scheme. Additionally, it has been reported that the growth of graded layers would create a pseudomorphic thick InGaN with low crystallographic defects, which is of great benefit to the subsequent growth of intrinsic absorption layer, and the enhanced power conversion efficiency of the device [23]. Since the polarization charges within each unit cell are identical and uniform, smooth spatial variation of potential profile without an introducing of band offset is expected, facilitating high-efficient transportations and collections of photogenerated carriers in both lateral and vertical directions.

We simulated the polarization-induced III-nitride n-i-p solar cells by using the semiconductor finite element analysis software APSYS, which self-consistently solves the Poisson and Schrödinger equations, and allows for composition dependent material parameters. The material parameters of GaN and InN alloys such as the dielectric constant, electron (hole) effective mass, electron affinity, and minority electron (hole) lifetime adopted in this work can be found in [24]. The $In_xGa_{1-x}N$ alloy properties were determined by using a linear interpolation between GaN and InN alloys. The wavelength-dependent refractive index and absorption coefficient for

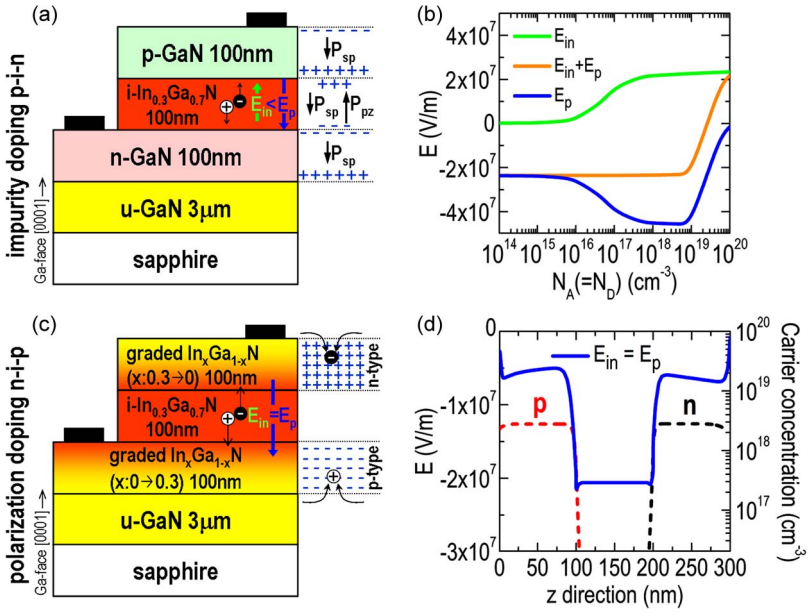

Fig. 2. (a) Conventional solar cell structure used as a reference device and (b) its built-in (E_{in}) and polarization-induced (E_P) electric fields within the $In_{0.3}Ga_{0.7}N$ absorption layer versus doping concentrations of p- and n-GaN layers ($N_A = N_D$). (c) The proposed structure of polarization-induced doping n-i-p solar cell and (d) the corresponding polarization-induced doping density and electric filed along the growth direction of the device.

$In_xGa_{1-x}N$ were taken into account [25], and the temperature-dependent electron and hole mobility substituted for both impurity doping and polarization-induced doping solar cells were also considered [16], [26]. It should be noted that as the experimental value of surface charges is generally lower than that of the theoretical one due to the screening of epitaxial defects and indium segregations [27], we therefore set 50% of the theoretical value to demonstrate the effect of polarization charges in this work.

2.2. Device Structure

Fig. 2(a) shows the conventional solar cell structure for a reference in this study, which was grown on a c-plane sapphire substrate, followed by a 3-μm-thick undoped GaN buffer layer and a typical p-i-n structure, consisting of a 100-nm-thick n-type GaN, a 100-nm-thick intrinsic $In_{0.3}Ga_{0.7}N$ absorption layer, and a 100-nm-thick p-type GaN. Fig. 2(b) plots its built-in (E_{in}) and polarization-induced (E_P) electric fields within the $In_{0.3}Ga_{0.7}N$ absorption layer versus doping concentrations of p- and n-GaN layers ($N_A = N_D$). The net electric field, $E_{in} + E_P$, is also plotted in the figure. Accordingly, E_{in} and E_P are in the opposite direction (E_{in} points from n- to p-type GaN layers along the [0001] direction, while E_P of Ga-face polarity wurtzite crystal points along the $[000\bar{1}]$ direction), and $|E_P|$ is generally larger than $|E_{in}|$ for the doping concentrations of $N_{A,D} \leq 1 \times 10^{19}$ cm^{-3}. Therefore, the net electric field will move photogenerated carriers created by light absorption of intrinsic $In_{0.3}Ga_{0.7}N$ layer in a detrimental way (i.e., electrons to p-GaN, while holes to n-GaN) as plotted in Fig. 2(a), making it impossible for carrier collection and diminishing the photocurrent of the device. By further increasing the doping concentrations to $N_{A,D} > 1 \times 10^{19}$ cm^{-3}, E_P decreases rapidly as the piezoelectric polarization sheet charges are screened by highly doped GaN regions on either side of the $In_{0.3}Ga_{0.7}N$ absorption layer. After that, E_{in} starts dominating the net eclectic filed of the device, which renovates the potential profile of the $In_{0.3}Ga_{0.7}N$ absorption layer for efficient carrier collections. However, such highly impurity-based doping concentrations ($> 1 \times 10^{19}$ cm^{-3}) are difficult to achieve, especially in p-type GaN due to its inefficient thermal activation of dopant acceptors.

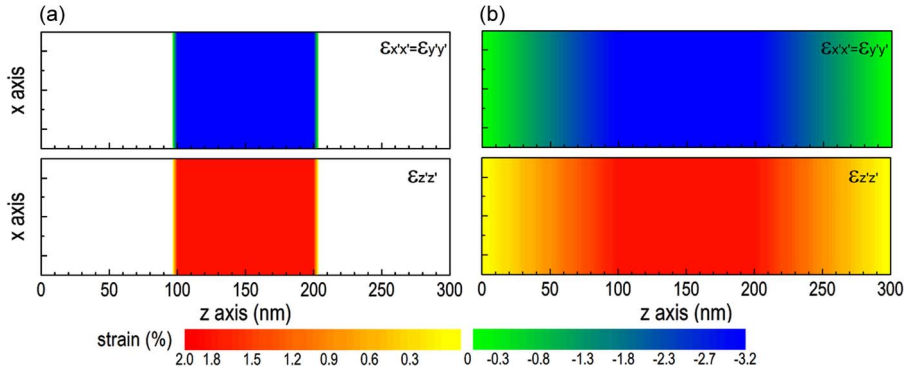

Fig. 3. Calculated strain profile in the $x\ (=y)$ and z direction of (a) impurity doping p-i-n and (b) polarization-induced doping n-i-p solar cells.

For the improved structure [see Fig. 2(c)], the original 100-nm-thick p- and n-type GaN layers are replaced by the 100-nm-thick graded $In_xGa_{1-x}N$ layers, where the indium compositions are linearly grading from $x = 0\%$ to $x = 30\%$ and back to 0% to construct the p- and n-type regions of the solar cell. As plotted in Fig. 2(c), the negative polarization charge field created by grading $In_xGa_{1-x}N$ layer $(GaN \rightarrow In_{0.3}Ga_{0.7}N)$ attracts holes to realize p-type doping in the bottom of the device. Meanwhile, as a result of attracting holes, negative charges (electrons) are hence supplied to the positive polarization charge filed induced by reversely grading $In_xGa_{1-x}N$ layer $(In_{0.3}Ga_{0.7}N \rightarrow GaN)$, resulting in the Fermi level close to the conduction band and defining an n-type conducting region in the top of the device. While the light absorption layer of the improved device is kept the same as that of the conventional III-nitride p-i-n solar cell. Most importantly, in the absence of any impurity doping, such device's built-in electric field across the $In_{0.3}Ga_{0.7}N$ absorption layer actually is equivalent of its polarization-induced electric field $(E_{in} = E_P)$, beneficial for the electric drifting and efficient collection of photogenerated carriers. Fig. 2(d) shows the polarization-induced doping density and electric filed along the growth direction of the improved device. Accordingly, the distributed profiles of field-ionized carriers (red dash-line for holes; black dash-line for electrons) are symmetrical, and a high carrier density of $p = n = 3 \times 10^{18}$ cm^{-3} is achievable by using polarization-doping scheme. As the polarization charge is uniformly built into the unit cell, the polarization-doping profiles are precisely controlled and well defined within the graded $In_xGa_{1-x}N$ regions, and that is difficult to achieve by random impurity doping due to the segregation or diffusion tendencies of acceptors and donors [28]. The magnitude of E_{in} $(= E_P)$ within the $In_{0.3}Ga_{0.7}N$ absorption layer is around 2×10^7 V/m. As plotted in Fig. 2(b), the conventional III-nitride p-i-n device would achieve a similar value of electric field; however, the doping concentrations must be as high as $N_{A,D} \sim 10^{20}$ cm^{-3} to efficiently screen the E_P, and again, that is unrealistic for the MOCVD growth.

3. Results and Discussion

Fig. 3 depicts the strain profiles in the x (equal to y) and z directions for (a) the impurity doping p-GaN/i-$In_{0.3}Ga_{0.7}N$/n-GaN and (b) polarization-induced doping n-i-p solar cells. The GaN layer is assumed to be relaxed, and the $In_xGa_{1-x}N$ layers are pseudomorphically grown on it. The calculation detail of strained nitride layers is described in [29]. The strain values are used to compute the piezoelectric polarization of the devices. As shown in Fig. 3(a), abrupt strain differences along both basal and z directions are observed at the GaN/$In_{0.3}Ga_{0.7}N$ hetero-interfaces, where the polarization-induced surface charges start accumulating. Consequently, the energy band of $In_{0.3}Ga_{0.7}N$ absorption layer is severely tilted, addressing the band discontinuities at GaN/$In_{0.3}Ga_{0.7}N$ hetero-interfaces. In contrast, the strain difference between the $In_{0.3}Ga_{0.7}N$ absorption layer and its contiguous layers is alleviated profoundly in the polarization-induced doping n-i-p device [see Fig. 3(b)], as do the accumulation of polarization-induced surface

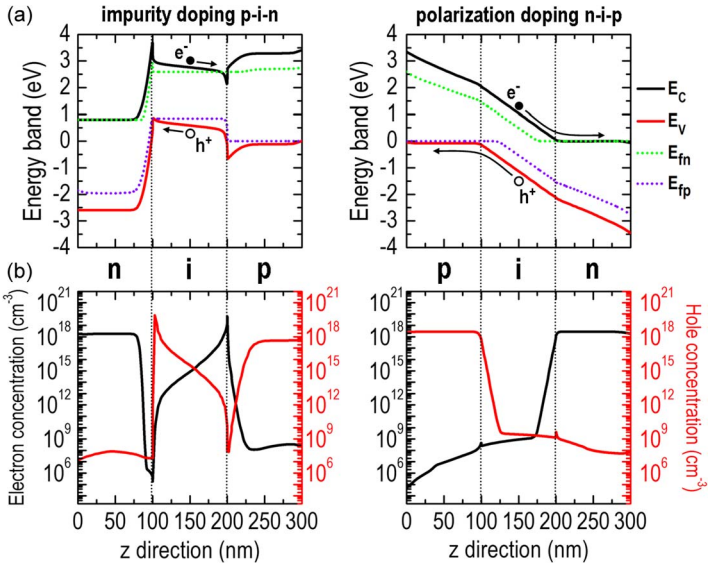

Fig. 4. Calculated (a) energy band diagrams and (b) distributions of photogenerated carriers (red line for holes and black line for electrons) for both impurity doping p-i-n ($p = 5 \times 10^{17}$ cm^{-3}, and $n = 5 \times 10^{18}$ cm^{-3}) and polarization-induced doping n-i-p solar cells under 1-sun illumination.

charges and the formation of piezoelectric field. The field-ionized carriers induced by grading $In_xGa_{1-x}N$ layers therefore determines the electric filed (directing from n-type to p-type) across the $In_{0.3}Ga_{0.7}N$ absorption layer, and that tilts the energy band in a favorite way for carrier collection, and simultaneously eliminates the band discontinuities at hetero-interfaces.

We now examine the physical effect of polarization-induced doping on the enhancement of carrier collection. Fig. 4(a) shows calculated energy band diagrams of the impurity doping p-i-n ($p = 5 \times 10^{17}$ cm^{-3}, and $n = 5 \times 10^{18}$ cm^{-3}) and polarization-induced doping n-i-p solar cells under 1-sun illumination. A sharp conduction and valence band offsets can be seen at hetero-interfaces for the impurity doping p-i-n structure, hindering the extraction of photogenerated carriers created in the $In_{0.3}Ga_{0.7}N$ absorption layer out of the device. Additionally, the band tilting of $In_{0.3}Ga_{0.7}N$ absorption layer is still detrimental for carrier drifting even under the illumination of solar light. As a result, the current generated in such an impurity doping p-i-n structure mainly attributes to the absorption in the GaN layers. As the improved device using polarization-doping scheme, a smooth potential profile without introducing discontinuities in both conduction and valence bands is observed, entirely due to the essential contribution of graded $In_xGa_{1-x}N$ regions. As previously discussed with reference to Fig. 3(b), the adverse impact of piezoelectric field on the band tilting of $In_{0.3}Ga_{0.7}N$ absorption layer is also alleviated, and the extraction of photogenerated carriers created by $In_{0.3}Ga_{0.7}N$ absorption layer outside the device hence becomes feasible. Therefore, as plotted in Fig. 4(b), most of photogenerated carriers in impurity doping p-i-n solar cell are accumulated and eventually vanished at hetero-interfaces, while our polarization-doping n-i-p structure contributes stable output of photocurrents.

Fig. 5 shows the temperature-dependent (50–400 K) J–V curves for (a) impurity doping p-i-n and (b) polarization-induced doping n-i-p solar cells. The power conversion efficiency (η) versus reciprocal temperature $(1/T)$ was also inserted in the figures. The short-circuit current (J_{SC}) of the impurity doping p-i-n solar cell decreases when temperature is lowered from 400 to 50 K [Fig. 5(a)], which is explained by the freezeout of thermally activated impurity dopants. While the device's open-circuit voltage (V_{OC}) actually increases with the decreasing temperature, it is mainly attributed to the enlarged size of energy band-gap of $In_{0.3}Ga_{0.7}N$ absorption layer. Consequently, an extremely low power conversion efficiency of $\eta \sim 0.1\%$ is generally obtained in impurity doping p-i-n solar cells under all temperatures. In comparison, the J_{SC} values of polarization-induced doping n-i-p solar cell are essentially independent of temperature, which is

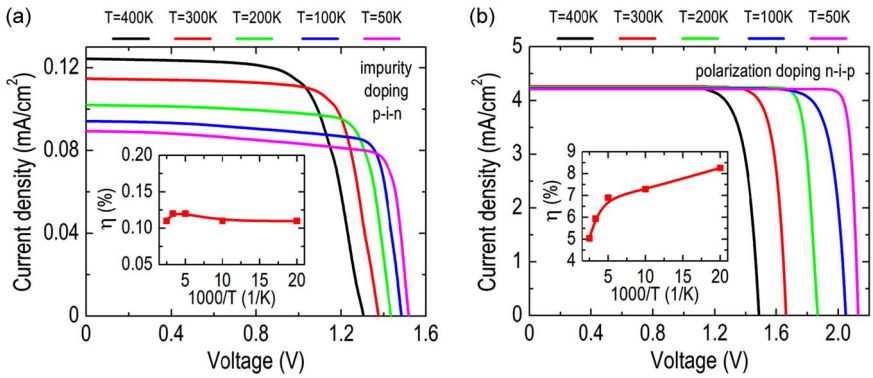

Fig. 5. Temperature-dependent (50–400 K) J–V curves of (a) impurity doping p-i-n and (b) polarization-induced doping n-i-p solar cells. The power conversion efficiency (η) versus reciprocal temperature $(1/T)$ was also inserted in the figures.

an indicative feature of field ionization as polarization charges are originally atomic and do not need thermal energy to be activated. With temperature variations, the calculated J_{SC} values are near identical to $J_{SC} \sim 4.3$ mA/cm^2, which is more than one order of magnitude enhancement as compared to that of impurity doping p-i-n solar cells. Again, the increasing of device's V_{OC} with decreasing temperature is primarily due to the enlarged energy band-gap of light absorption layer. Hence, a highest power conversion efficiency of $\eta \sim 8.5\%$ can be achieved on our polarization-induced doping n-i-p solar cell at the temperature of $T = 50$ K.

4. Conclusion

In conclusion, we propose a new type of III-nitride n-i-p solar cell not formed by impurity doping. The approach of polarization-induced doping is particularly useful for III-nitride solar cells with high indium contents in the $In_xGa_{1-x}N$ absorption layer as the band discontinuity at hetero-interfaces is considerably alleviated. Most importantly, as polarization charges are atomic in origin and do not need thermal energy to be activated, the short-circuit current of the proposed polarization-induced doping n-i-p solar cell is essentially independent of temperature and contribute to a high power conversion efficiency, which offers great potential for the next generation of photovoltaic cells.

References

[1] O. Jani, I. Ferguson, C. Honsberg, and S. Kurtz, "Design and characterization of GaN/InGaN solar cells," *Appl. Phys. Lett.*, vol. 91, no. 13, Sep. 2007, Art. ID. 132117.
[2] J.-K. Sheu *et al.*, "Demonstration of GaN-based solar cells with GaN/InGaN superlattice absorption layers," *IEEE Electron Device Lett.*, vol. 30, no. 3, pp. 225–227, Mar. 2009.
[3] J. Liu, Y. Zhou, J. Zhu, K. M. Lau, and K. J. Chen, "AlGaN/GaN/InGaN/GaN DH-HEMTs with an InGaN notch for enhanced carrier confinement," *IEEE Electron Device Lett.*, vol. 27, no. 1, pp. 10–12, Jan. 2006.
[4] Y.-L. Tsai *et al.*, "Improving efficiency of InGaN/GaN multiple quantum well solar cells using CdS quantum dots and distributed Bragg reflectors," *Solar Energy Mater. Solar Cells*, vol. 117, pp. 531–536, Oct. 2013.
[5] Y. Zhang *et al.*, "The effect of dislocations on the efficiency of InGaN/GaN solar cells," *Solar Energy Mater. Solar Cells*, vol. 117, pp. 279–284, Oct. 2013.
[6] Y.-J. Lee, M.-H. Lee, C.-M. Cheng, and C.-H. Yang, "Enhanced conversion efficiency of InGaN multiple quantum well solar cells grown on a patterned sapphire substrate," *Appl. Phys. Lett.*, vol. 98, no. 26, Jun. 2011, Art ID. 263504.
[7] Y.-C. Yao *et al.*, "Efficient collection of photogenerated carriers by inserting double tunnel junctions in III-nitride p-i-n solar cells," *Appl. Phys. Lett.*, vol. 103, no. 19, Nov. 2013, Art. ID. 193503.
[8] Y.-J. Lee *et al.*, "Slanted n-ZnO/p-GaN nanorod arrays light-emitting diodes grown by oblique-angle deposition," *APL Mater.*, vol. 2, no. 5, May 2014, Art. ID. 056101.
[9] J. J. Wierer, A. J. Fischer, and D. D. Koleske, "The impact of piezoelectric polarization and nonradiative recombination on the performance of (0001) face GaN/InGaN photovoltaic devices," *Appl. Phys. Lett.*, vol. 96, no. 5, 2010, Art. ID. 051107.
[10] C. J. Neufeld *et al.*, "Effect of doping and polarization on carrier collection in InGaN quantum well solar cells," *Appl. Phys. Lett.*, vol. 98, no. 24, 2011, Art. ID. 243507.

[11] H. Xing *et al.*, "Memory effect and redistribution of Mg into sequentially regrown GaN layer by metalorganic chemical vapor deposition," *Jpn. J. Appl. Phys.*, vol. 42, no. 1, pp. 50–53, Jan. 2003.
[12] A. G. Bhuiyan, K. Sugita, A. Hashimoto, and A. Yamamoto, "InGaN solar cells: Present state of the art and important challenges," *IEEE J. Photovoltaics*, vol. 2, no. 3, pp. 276–293, Jul. 2012.
[13] S. J. Pearton *et al.*, "Review of radiation damage in GaN-based materials and devices," *J. Vac. Sci. Technol. A, Vacuum, Surfaces, Films*, vol. 31, no. 5, pp. Sep. 2013, Art. ID. 050801.
[14] C. J. Eiting, P. A. Grudowski, and R. D. Dupuis, "Growth of low resistivity p-type GaN by metal organic chemical vapour deposition," *Electron. Lett.*, vol. 33, no. 23, pp. 1987–1989, Nov. 1997.
[15] W. Götz, N. M. Johnson, J. Walker, D. P. Bour, and R. A. Street, "Activation of acceptors in Mg-doped GaN grown by metalorganic chemical vapor deposition," *Appl. Phys. Lett.*, vol. 68, no. 5, pp. 667–669, Jan. 1996.
[16] J. Simon, V. Protasenko, C. Lian, H. Xing, and D. Jena, "Polarization-induced hole doping in wide-band-gap uniaxial semiconductor heterostructures," *Science*, vol. 327, no. 5961, pp. 60–64, Jan. 2010.
[17] S. D. Carnevale *et al.*, "Polarization-induced pn diodes in wide-band-gap nanowires with ultraviolet electroluminescence," *Nano Lett.*, vol. 12, no. 2, pp. 915–920, 2012.
[18] S. Li *et al.*, "Polarization induced pn-junction without dopant in graded AlGaN coherently strained on GaN," *Appl. Phys. Lett.*, vol. 101, no. 12, Sep. 2012, Art. ID. 122103.
[19] A. Nakajima, Y. Sumida, M. H. Dhyani, H. Kawai, and E. M. S. Narayanan, "GaN-based super heterojunction field effect transistors using the polarization junction concept," *IEEE Electron Device Lett.*, vol. 32, no. 4, pp. 542–544, Apr. 2011.
[20] S. Helkman *et al.*, "Polarization effects in AlGaN/GaN and GaN/AlGaN/GaN heterostructures," *J. Appl. Phys.*, vol. 93, no. 12, Jun. 2003, Art. ID. 10114.
[21] J. P. Ibbetson *et al.*, "Polarization effects, surface states, and the source of electrons in AlGaN/GaN heterostructure field effect transistors," *Appl. Phys. Lett.*, vol. 77, no. 2, pp. 250–252, Jul. 2000.
[22] I. Ho and G. B. Stringfellow, "Solid phase immiscibility in GaInN," *Appl. Phys. Lett.*, vol. 69, no. 18, pp. 2701–2703, Oct. 1996.
[23] S. Y. Bae *et al.*, "Pseudomorphic thick InGaN growth with a grading interlayer by metal organic chemical vapor deposition for InGaN/GaN p-i-n solar cells," *J. Crystal Growth*, vol. 387, pp. 23–28, Feb. 2014.
[24] G. F. Brown, J. W. Ager, W. Walukiewicz, and J. Wu, "Finite element simulations of compositionally graded InGaN solar cells," *Solar Energy Mater. Solar Cells*, vol. 94, no. 3, pp. 478–483, Mar. 2010.
[25] W. Walukiewicz *et al.*, "Structure and electronic properties of InN and In-rich group III-nitride alloys," *J. Phys. D, Appl. Phys.*, vol. 39, no. 5, pp. R83–R99, Mar. 2006.
[26] D. Jena *et al.*, "Realization of wide electron slabs by polarization bulk doping in graded III-V nitride semiconductor alloys," *Appl. Phys. Lett.*, vol. 81, no. 23, pp. 4395–4397, Dec. 2002.
[27] O. Mayrock, H. J. Wunsche, and F. Henneberger, "Polarization charge screening and indium surface segregation in (In,Ga)N/GaN single and multiple quantum wells," *Phys. Rev. B*, vol. 62, Dec. 2000, Art. ID. 16870.
[28] B. Y. Ber *et al.*, "Secondary ion mass spectroscopy investigations of magnesium and carbon doped gallium nitride films grown by molecular beam epitaxy," *Semicond. Sci. Technol.*, vol. 13, no. 1, pp. 71–74, Jan. 1998.
[29] A. E. Romanov, T. J. Baker, S. Nakamura, J. S. Speck, ERATO/JST UCSB Group, "Strain-induced polarization in wurtzite III-nitride semipolar layers," *J. Appl. Phys.*, vol. 100, 2006, Art. ID. 023622.